

# UAV Icing: Comparison of LEWICE and FENSAP-ICE for Ice Accretion and Performance Degradation

Richard Hann<sup>1</sup>

Norwegian University of Science and Technology (NTNU), Trondheim, 7034, Norway

One of the main limitations of the operational envelope of UAVs today is the risk of atmospheric icing. UAV icing is not well researched and this paper aims to generate a better understanding of how ice accretion and aerodynamic performance degradation on UAV airfoils can be simulated. In particular, the objective is to investigate how well a panel-method based code compares to a modern CFD icing code. LEWICE and FENSAP-ICE are used to generate three characteristic 2D ice shapes (rime, glaze, mixed) on a NREL S826 airfoil for low Reynolds numbers. RANS calculations are performed to assess the resulting aerodynamic performance degradation. Validation of the ice growth predictions is achieved by using literature data. Aerodynamic performance degradation is validated with experimental results from a (non-icing) wind tunnel at NTNU. The numerical results indicate that icing morphology has a major influence on the ability of both codes to capture ice shape and aerodynamic penalties. Rime is simulated consistently, whereas predictions for mixed and glaze show significant differences. All ice cases negatively impact the aerodynamic performance by reducing maximum lift, decreasing stall angle and increasing drag.

## I. Nomenclature

$\alpha$	=	angle of attack
$c$	=	chord
$c_d$	=	drag coefficient
$c_l$	=	lift coefficient
$k_s$	=	equivalent sand-grain roughness
$LWC$	=	liquid water content
$MVD$	=	droplet median volume diameter
$Re$	=	Reynolds number
$T$	=	temperature
$t$	=	time
$v$	=	velocity

## II. Introduction

Over the past years, the utilization of unmanned aerial vehicles (UAVs) has drastically increased for a wide range of applications. In particular, small fixed-wing UAVs, with wing spans of a few meters have been developed for a multitude of autonomous air-borne tasks. Today, the operation envelope of these UAVs is significantly limited by atmospheric icing. Due to a lack of effective icing protections systems, UAVs are usually grounded when icing conditions are expected. The objective of this work is to increase the understanding of the effects of icing on UAV aerodynamic performance by comparing two numerical methods.

Atmospheric in-cloud icing affects all types of airborne vehicles and has therefore been in the focus of research for several decades aimed at commercial and military aircrafts. Hence today, there is a well-established understanding of iced-airfoil aerodynamics for subsonic aviation [1]. However, surprisingly little research has been performed in the field of UAV icing, although the significant risk of atmospheric icing on UAV operations has been already described in the early 1990s [2]. The findings from commercial and military icing research cannot directly be transferred to UAVs due to the difference in the Reynolds number regime. Most of the existing icing research has been performed

---

<sup>1</sup> PhD Candidate, Norwegian University of Science and Technology, Centre for Autonomous Marine Operations and Systems (NTNU-AMOS), O. S. Bragstads plass 2D, 7034 Trondheim, Norway

at relatively high Reynolds numbers  $Re = 1 \dots 10 \times 10^6$ . In contrast, UAVs typically operate in the low Reynolds regime  $Re = 1 \dots 10 \times 10^5$ , due to lower flight velocities and smaller airframe sizes compared to commercial or military aircrafts. This implies that dedicated research for icing phenomena on UAVs has a high relevance.

Several research groups already performed significant contributions on the topic of UAV icing using different approaches. The impact of the Reynolds number on icing has been covered by Szilder and McIlwain [3] implementing a morphogenetic icing model [4]. The same model has also been used to investigate the aerodynamic performance degradation on 2D airfoils and 3D swept wings [5, 6]. Koenig, Ryerson, and Kmiec have applied the NASA code LEWICE to assess icing impact on a 2D UAV airfoil [7]. FENSAP-ICE is another widely used icing simulation tool that has been applied to investigate the effect of icing on UAVs in 2D and 3D [8, 9]. Results from LEWICE in combination with the flow solver module of FENSAP-ICE have been implemented in a flight simulator to investigate the impact of ice on UAVs [10].

The objective of this study is to investigate ice growth and consequent performance degradation on a 2D UAV airfoil. With the availability of several icing tools, there is a need to compare the different codes to each other. Similar work has been already performed for aircraft applications by Pueyo, Brette, Vafa and Akel [11].

### III. Methods

Two numerical tools will be used to predict ice shapes on a 2D airfoil. LEWICE (version 3.2.2) is a widely used first generation ice accretion tool based on a 2D panel-method [14]. LEWICE has been developed by NASA and has been validated over a wide range of parameters with extensive experimental icing wind tunnel data [15]. LEWICE is formally only validated in a high Reynolds number regime ( $Re > 2.3 \times 10^6$ ) [14], but it may still be practically used for lower Reynolds numbers. The 2D panel-method in LEWICE has very low computational requirements which allows LEWICE to obtain a large number of results in a short time. This feature is well suited to study a wide range of icing parameters to gain a better understanding of the dominating variables in a specific icing scenario. Such a characteristic is particularly relevant for designing an efficient icing protection system with regards to investigating different cases, configurations, heat requirements, etc. However, because a panel-method captures many of the physical processes by means of correlation and calibration, the results for the ice growth need to be compared to a code with a higher order of accuracy.

FENSAP-ICE is a second generation, state-of-the-art icing code capable of 2D and 3D icing simulations for a large variety of applications [9]. The code consist of separate modules that aim to capture the main physical icing processes [16]: the flow field is simulated with a Reynolds-Averaged Navier-Stokes (RANS) flow solver; droplet and ice crystal impingement are simulated using an Eulerian approach; ice growth is captured by solving the partial differential equations (PDEs) on the iced geometry. In addition, FENSAP-ICE includes a powerful re-meshing engine

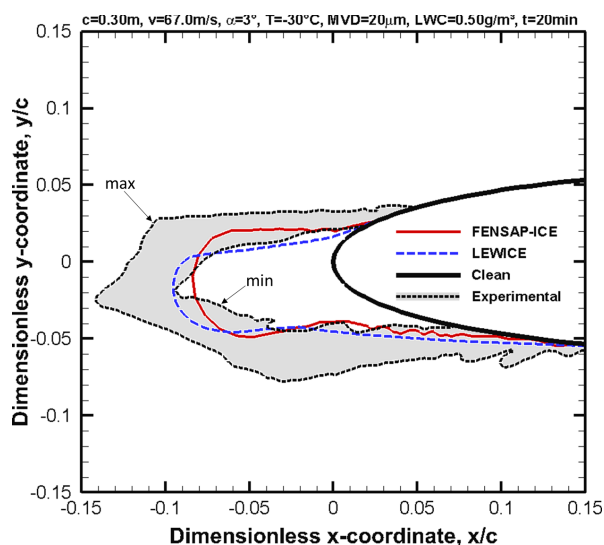


Fig. 1. Simulation results for FENSAP-ICE and LEWICE compared to experimental rime ice (min/max) on NACA0012 [12],  $Re = 1.9 \times 10^6$ .

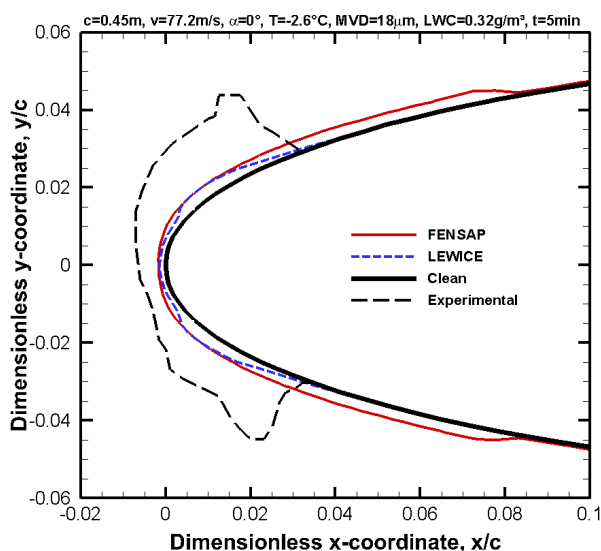


Fig. 2. Simulation results for FENSAP-ICE and LEWICE to experimental glaze ice on NACA0012 [13],  $Re = 2.7 \times 10^6$ .

that adapts the grid to the iced geometry. To simulate ice growth, these modules are run iteratively in a multi-step process. In this study, it will be assumed that FENSAP-ICE results have a higher degree of fidelity compared to LEWICE, because FENSAP-ICE implements higher order models for resolving physical processes. However, it is still acknowledged that compared to reality, FENSAP-ICE results may deviate substantially, particularly for low Reynolds numbers and challenging icing conditions.

Three icing cases are investigated in this study, which are presented in Table 1. They have been selected from a large number of LEWICE iterations aimed to find representative ice shapes for three main ice morphologies: glaze, mixed and rime [17]. Rime ice occurs at low temperatures when the super-cooled cloud droplets freeze immediately when colliding with an object. Glaze is forming at temperatures close to freezing when the majority of impacting droplets form a water film on the surface that is gradually turning into ice. Mixed is a combination of these two cases and often exhibits large horn formations.

Ice accretion cases are in general defined by the following parameters: free stream icing velocity  $v_{icing}$ , duration of icing  $t_{icing}$ , airfoil chord length  $c$ , angle of attack  $\alpha_{icing}$ , liquid water content  $LWC$ , median volume diameter  $MVD$ , ambient temperature  $T_{icing}$  and equivalent sand-grain surface roughness  $k_s$ . Flight velocities are chosen according to typical cruise speeds of small scale UAVs, with the exception for mixed ice which was selected to obtain a distinct horn formation. The liquid water content is selected according to 14 CFR Part 25, Appendix C for continuous maximum icing conditions [19]. The surface roughness is estimated using empirical correlations [20]. The NREL S826 airfoil is a high lift-to-drag ratio foil with an insensitivity to transition [21]. The airfoil is suited for long-endurance UAV designs as well as wind turbine blades at low Reynolds numbers.

LEWICE and FENSAP-ICE are used to generate ice shapes according to Table 1. For the assessment of the aerodynamic performance degradation due to icing, the CFD module in FENSAP-ICE is used to simulate the flow field around the iced geometries from both codes. This is applied due to the nature of the panel-method in LEWICE, which fails to accurately predict lift and drag in the presence of separation at leading-edge ice horns. All CFD calculations are performed by using a steady-state Spalart-Allmaras turbulence model and a streamline upwind artificial viscosity model. The discretization for CFD is executed as hybrid O-grids with structured resolution of the boundary layer.

**Table 1. Icing test cases.**

Parameter	Icing Type		
	Glaze	Mixed	Rime
Velocity $v_{icing}$	25 m/s	40 m/s	25 m/s
Icing duration $t_{icing}$	40 min		
Angle of attack $\alpha_{icing}$	0°		
Chord $c$	0.45m		
Droplet $MVD$	30 $\mu\text{m}$	20 $\mu\text{m}$	20 $\mu\text{m}$
Liquid water content $LWC$	0.34 g/m <sup>3</sup>	0.55 g/m <sup>3</sup>	0.54 g/m <sup>3</sup>
Temperature $T_{icing}$	-2 °C	-5 °C	-10 °C
Roughness $k_s$	0.6 mm	1 mm	1 mm

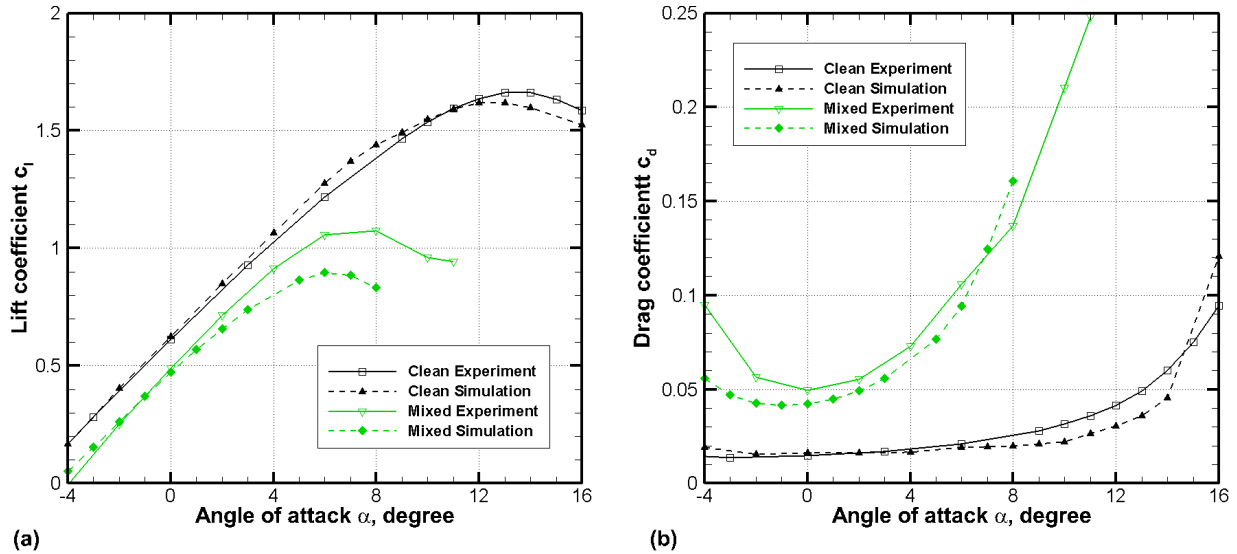


**Fig. 3. Comparison of lift (a) and drag (b) results between wind tunnel experiments [18] and simulation data for clean and LEWICE-mixed,  $Re = 4 \times 10^5$ .**

#### IV. Validation

The validation of the simulation set-up consists of two independent steps. The first step is to validate the ice accretion model of the codes for low Reynolds numbers. Unfortunately, at this point there are no experimental icing data available for the low Reynolds and Mach number regime of UAVs [5]. Therefore, a literature search has been performed to identify potentially suitable icing cases for validation. Following Szilder and Yuan [5], the experimental rime results from an icing wind tunnel interfacility test [12] on a NACA0012 airfoil at  $Re = 1.9 \times 10^6$  seemed appropriate for comparison. Figure 1 shows the results from this work for LEWICE and FENSAP-ICE and the minimum and maximum extent of the experimental ice shapes obtained during the interfacility test. Note the significant spread (grey area) of the wind tunnel data. The predicted ice shapes from LEWICE and FENSAP-ICE both land reasonably within the range of experimental results. It can be noticed though, that FENSAP-ICE estimates a lower icing area and ice horn extent. Both LEWICE and FENSAP-ICE show an under-prediction of the upper icing limit. In general, it can be noticed that both ice shapes appear to be more regular and smooth compared to the experimental results. Consequently, this is expected to result in overly optimistic aerodynamic performance degradation predictions.

An experimental glaze ice shape from the NATO RTO Technical Report 38 [13] (case C-4) is also used for validation and shown in Fig. 2. Both icing codes seemingly fail to capture the experimental glaze geometry. Neither of the codes exhibit the T-shaped ice horn from the wind tunnel. Instead, the ice accretion is smooth with significantly lower ice extent and ice area. The LEWICE ice limits match the experiment well, whereas FENSAP-ICE predicts ice limits substantially further downstream. This icing case has been proven as challenging throughout the NATO report [13] where all codes performed poorly. Szilder and McIlwain also obtained a low similarity for this case [3]. There are two possible explanations for this situation. On the one hand, glaze is the most difficult icing type to capture due to the complex thermodynamic surface processes. Hence, this validation case could indicate that all codes are limited in their capability to simulate glaze. On the other hand, the results of the icing tunnel interfacility test [12] demonstrate that experimental data can exhibit a large range of uncertainty and variability (see example in Fig. 1). This means that the large deviations observed in the glaze validation case may be related to experimental ambiguity. In addition, the ice accretion rate is driven by velocity whereas total ice mass is driven by duration [22]. Flight velocities for UAVs are typically significantly lower with longer icing durations compared to the validation cases. All these factors limit the overall validity of the presented validation cases but need to be accepted in absence of appropriate experimental data at low Reynolds numbers.

The second step of the validation is to confirm that the FENSAP-ICE CFD module is capable of accurately predicting lift and drag for iced geometries at low Reynolds numbers. For this task, experiments in the closed-loop low-speed wind tunnel at the Norwegian University of Science and Technology (NTNU) were conducted. Lift and drag measurements were conducted for the NREL S826 airfoil for both clean and iced conditions. Icing on the airfoil

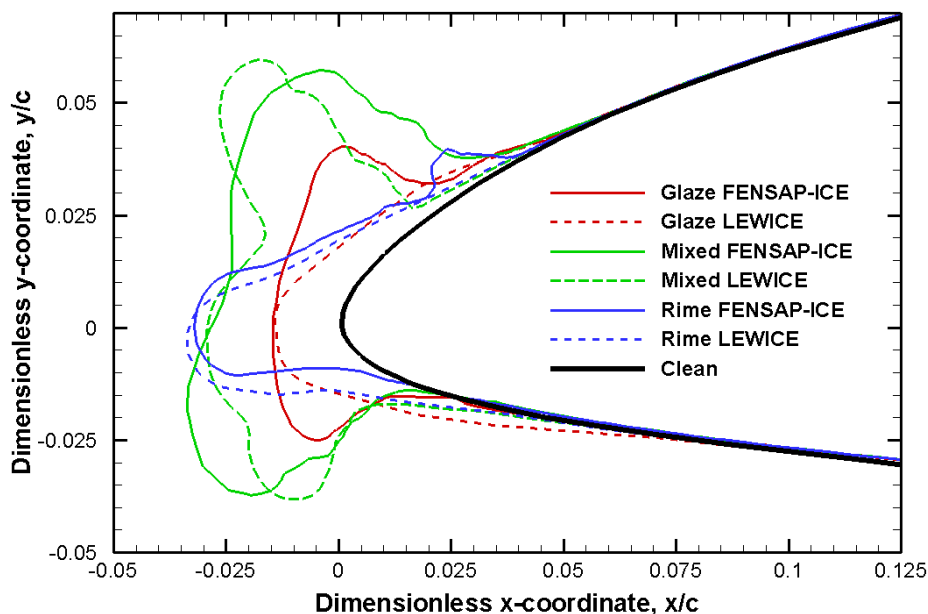


Fig. 4. Ice shape results with LEWICE and FENSAP-ICE for the test cases.

was imitated by attaching 3D printed ice edges on the clean airfoil. Artificial ice shapes have been printed based on LEWICE simulation results (see Fig. 4 dashed lines) for the test cases in Table 1. The results of these wind tunnel experiments are not yet published but prepared for submission [18].

Figure 3a and 3b display experimental and numerical results for a clean airfoil and for a mixed ice geometry. The artificial ice shape is based on the LEWICE (mixed) and the aerodynamic coefficients are obtained with the FENSAP-ICE flow solver. The mixed ice case is chosen as it imposes the strongest disturbances to the flow, by introducing leading-edge separation.

The comparison of the lift coefficients in Fig. 3a show that the numerical results are in good correspondence with the experimental data. Differences for the clean case are most likely related to inadequate transition modeling. The mixed ice results overlap well in the linear region. For higher angles of attack the discrepancies between the numerical and experimental curve increase, which may be linked to the turbulence modeling. Stall angle and maximum lift are both underpredicted by the numerical method. Figure 3b displays that drag is reasonably well modeled in all cases. A minor exception can be detected at the higher and lower limit of angle of attack for the iced case. This deviation between the numerical and experimental data is most likely connected to the complex leading-edge separation turbulence modeling.

## V. Ice Shape Results

Figure 4 shows the resulting ice shapes for LEWICE and FENSAP-ICE for the cases specified in Table 1. Rime ice shows the largest similarity between the two codes. The ice extent, direction, area and overall shape match well, although three dissimilarities can be detected. The lower icing limit for LEWICE is predicted at about  $x/c = 0.05$  which is further downstream compared to FENSAP-ICE at  $x/c = 0.02$ . In addition, the FENSAP-ICE solution exhibits an ice bump on the upper side for which no trace can be found in LEWICE. Lastly, there seems to be a small difference in the ice horn angle.

The glaze results display significant differences between the two icing codes. The LEWICE glaze ice shape looks comparable to the rime result, with a conical ice horn. FENSAP-ICE predicts a much more complex T-shaped ice structure. For glaze as well, the lower icing limit in LEWICE ( $x/c = 0.08$ ) is further downstream compared to FENSAP-ICE ( $x/c = 0.03$ ). The maximal ice extent is almost identical for both codes, but the ice area in FENSAP-ICE is approximately 40% larger, indicating higher collection rates.

Large differences can be also observed for the mixed ice case. The LEWICE results come in a tridentic-shape with a very distinct upper horn whereas the FENSAP-ICE mixed ice shape resembles a V-shape tail. LEWICE icing limits on both on the upper and lower side are upstream ( $\Delta x/c = 0.02$ ) compared to FENSAP-ICE. The total ice area is approximately 20% larger for FENSAP-ICE.

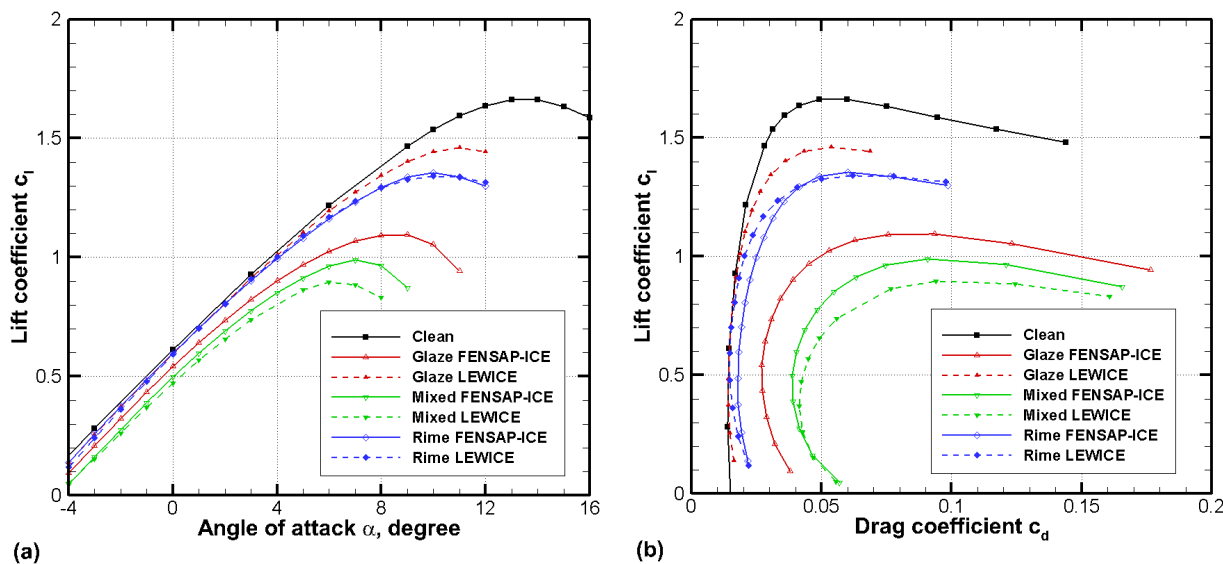


Fig. 5. Aerodynamic performance degradation for lift (a) and drag (b) based on numerical results for the FENSAP-ICE and LEWICE ice shapes,  $Re = 4 \times 10^5$ .

## VI. Aerodynamic Performance Degradation Results

The corresponding lift and drag coefficients for the ice shapes from Table 1 are presented in Fig. 5a and 5b. All ice shapes result in a degradation of aerodynamic performance by decreasing lift and increasing drag. In addition, the angle of maximum lift is reduced for all ice cases, increasing the stall risk and thus limiting the flight envelope.

The lift and drag curves for rime ice show a strong congruence between FENSAP-ICE and LEWICE. This was expected, as the rime ice shapes are very similar in geometry. The FENSAP-ICE rime shapes exhibit a higher drag, in particular in the linear region. This is likely to be explained by the small bump on the upper surface which is causing a small leading-edge separation bubble.

For mixed ice, the discrepancies in lift and drag are larger. The more curved LEWICE geometry results in stronger lift and drag penalties as well as an earlier stall onset. The differences are most distinct at higher angles of attack. The CFD results show that separation occurs for both codes at the upper and lower side of the leading-edge. In the LEWICE case, the pronounced upper horn leads to a stronger increase in turbulent intensity which is intensifying for at higher angles of attack.

The geometry of the glaze ice cases varies significantly between LEWICE and FENSAP-ICE. The LEWICE geometry is smooth and does not introduce significant disturbances in the boundary layer. This results in the lowest aerodynamic performance degradation of all ice cases. In contrast, the FENSAP-ICE geometry is more curved and horn-like, inducing flow separation at the leading-edge that lead to significantly larger performance penalties.

## VII. Discussion

The comparison between LEWICE and FENSAP-ICE ice shapes reflects the capabilities of the underlying numeric schemes. Both codes perform well for rime. This is likely explained by the simpler icing mechanics of rime where all incoming droplets freeze instantly. In contrast, the cases with a significant discrepancy between the two codes, are all governed by more complex thermodynamic processes.

Leading-edge separation occurs for all three icing cases in FENSAP-ICE. The intensity of the separation is varying, weakest for rime and strongest for mixed. The LEWICE panel-method is by design incapable to capture separation effects. This introduces an inherent error in LEWICE for the droplet collection efficiency, heat transfer and consequently on the ice accretion.

The impact of this error on the aerodynamic performance degradation is complex and depends on the ice morphology. For glaze, the LEWICE geometry is smooth and introduces only minimal disturbances to the flow. In contrast, the FENSAP-ICE glaze horn is more curved and induces significant flow separation at the upper and lower side of the leading edge. This results in disparate aerodynamic coefficients between the two codes. LEWICE estimates a minor penalty in lift and drag, whereas FENSAP-ICE predicts a decrease of lift (ca. 10%), a substantial increase of drag (ca. 90%) and a decrease of the stall angle. For mixed ice this behavior does not occur. Although there are considerable differences in the simulated ice shapes, the corresponding aerodynamic performance degradation is comparable, especially in the linear region. This highlights the sensitivity of performance loss to ice shape geometry. Complex geometries with high curvature that trigger separation will exhibit stronger flow disturbances and larger performance penalties.

## VIII. Conclusion

Numerical ice shape generation and simulation of aerodynamic performance degradation have been performed. The impact of icing on a UAV airfoil is studied for three icing cases at low Reynolds numbers. LEWICE is a 2D code based on a panel-method that has low computational requirements and may be used to run a larger number of simulations in a short time. A key question is if LEWICE can be used to perform parameter studies for UAV airfoils. To answer this, ice accretion and aerodynamic penalty predictions from LEWICE are compared with FENSAP-ICE. FENSAP-ICE is based on a Navier-Stokes solver with higher accuracy but also higher computational demands.

Three icing morphologies (rime, mixed and glaze) are investigated and compared between LEWICE and FENSAP-ICE. The resulting ice geometries are congruent for rime ice but deviate significantly for glaze and mixed ice. The most likely explanation is that in the latter two cases the icing mechanism is more complex and key flow features are not captured by the panel-method. This in consequence, has a detrimental influence on the performance degradation prediction. For rime, both codes give similar results whereas the discrepancies are larger for mixed and largest for glaze. The mixed ice geometries are disparate in geometry but the aerodynamic performance degradation level is still comparable. In contrast, for glaze the geometries are dissimilar as well as the aerodynamic penalties.

Generally, all cases show that icing decreases the aerodynamic performance of the UAV airfoil. Maximum lift and stall angle are decreased whereas drag is increased. The gradient of the lift curve in the linear region is not affected

significantly. The intensity of the disturbances is mainly depending on the ice shape and the occurrence of leading-edge separation.

In summary, the comparison between the two codes shows that LEWICE does have limitations. Icing cases with substantial amounts of non-freezing water are challenging to capture and may result in unrealistic and simplified ice shapes. Consequently, this means that the performance degradation is strongly dependent on the icing morphology. LEWICE seems suitable to investigate both ice accretion and aerodynamic performance degradation on UAVs for rime conditions. For glaze, the validity of the results may be very limited and should be handled with special care. Mixed icing seems to perform better but clear conclusions cannot be drawn at this stage.

Ideally, this work should be supported by validation with experimental results for low Reynolds numbers. However, at this time, no such data exists in the literature which means that a significant uncertainty remains. To mitigate this, there are ongoing preparations for conducting icing wind tunnel experiments at low Reynolds numbers. In absence of this data, validation of the ice accretion methods is performed with comparison data at moderately low Reynolds numbers. For rime ice, both codes perform well but for glaze both codes fail, which may also be related to experimental uncertainties and limitations. This underlines the necessity to perform further experimental investigations, especially for temperatures close to freezing and at low flow velocities.

The process of estimating performance degradation is validated by wind tunnel experiments at NTNU with artificial ice edges. The results indicate that the FENSAP-ICE flow solver perform reasonably well in predicting lift and drag coefficients of iced airfoils at low Reynolds numbers.

This work is limited by the fact that only three icing cases on a specific airfoil are investigated and the validation is performed at higher Reynolds numbers. Therefore, further research – numerically and especially experimentally – is required to gain a deeper understanding of the capabilities of LEWICE and FENSAP-ICE for low Reynolds numbers and UAV applications.

### Acknowledgements

This project has received funding from the Centre for Integrated Remote Sensing and Forecasting for Arctic Operations (CIRFA) under grant number 237906. The research was also funded by the Research Council of Norway through the Centres of Excellence funding scheme, grant number 223254 NTNU AMOS.

### References

- [1] Bragg, M. B., Broeren, A. P., and Blumenthal, L. A., “Iced-airfoil aerodynamics,” *Progress in Aerospace Sciences*, vol. 41, 2005, pp. 323–362.
- [2] Siquig, A., “Impact of Icing on Unmanned Aerial Vehicle (UAV) Operations,” Naval Environmental Prediction Research Facility report, PR 90:015:442, 1990.
- [3] Szilder, K., and McIlwain, S., “In-Flight Icing of UAVs - The Influence of Reynolds Number on the Ice Accretion Process,” SAE Technical Paper 2011-01-2572, 2011.
- [4] Szilder, K., and Lozowski, E., “Progress towards a 3D Numerical Simulation of Ice Accretion on a Swept Wing using the Morphogenetic Approach,” SAE Technical Paper 2015-01-2162, 2015.
- [5] Szilder, K., and Yuan, W., “The Influence of Ice Accretion on the Aerodynamic Performance of a UAS Airfoil,” *53rd AIAA Aerospace Sciences Meeting*, 2015, p. 536.
- [6] Szilder, K., and Yuan, W., “In-flight icing on unmanned aerial vehicle and its aerodynamic penalties,” *Progress in Flight Physics*, vol. 9, 2017, pp. 173–188.
- [7] Koenig, G. G., Ryerson, C. C., and Kmiec, R., “UAV Icing Flight Simulation,” *40th Aerospace Sciences Meeting & Exhibit*, Reno, Nevada: 2002.
- [8] Tran, P., Baruzzi, G., Tremblay, F., Benquet, P., Habashi, W. G., Petersen, P. B., Liggett, M. W., and Fiorucci, S., “FENSAP-ICE applications to unmanned aerial vehicles (UAV),” *42nd AIAA Aerospace Sciences Meeting and Exhibit*, 2004, pp. 390–402.
- [9] Habashi, W. G., Aubé, M., Baruzzi, G., Morency, F., Tran, P., and Narramore, J. C., “Fensap-Ice : a Fully-3D in-Flight Icing Simulation System for Aircraft , Rotorcraft and Uavs,” *24th International Congress of the Aeronautical Sciences*, 2004, pp. 1–10.
- [10] Hann, R., Wenz, A., Gryte, K., and Johansen, T. A., “Impact of Atmospheric Icing on UAV Aerodynamic Performance,” *Workshop on Research, Education and Development of Unmanned Aerial Systems (RED-UAS)*, Linköping: 2017.
- [11] Pueyo, A., Coentlin, B., Sherry, V., and Iyad, A., “A Comparison Exercise of Ice Accretion Simulations with 2D and 3D Solvers,” SAE Technical Paper 2007-01-3338, 2007.

- [12] Aerospace Information Report, "Icing Wind Tunnel Interfacility Comparison Tests," AIR5666, 2012.
- [13] NATO RTO Technical Report 38, "Ice Accretion Simulation Evaluation Test," RTO-TR-038 AC/323(AVT-006)TP/26, 2001.
- [14] Wright, W., "User's Manual for LEWICE Version 3.2," NASA/CR—2008-214255, 2008.
- [15] Wright, W., and Rutkowski, A., "Validation Results for LEWICE 2.0," NASA/CR—1999-208690, 1999.
- [16] Morency, F., Beaugendre, H., Baruzzi, G., and Habashi, W., "FENSAP-ICE - A comprehensive 3D simulation system for in-flight icing," *15th AIAA Computational Fluid Dynamics Conference*, 2001.
- [17] Lynch, F. T., and Khodadoust, A., "Effects of ice accretions on aircraft aerodynamics," *Progress in Aerospace Sciences*, vol. 37, 2001, pp. 669–767.
- [18] Hann, R., Brandrud, L., Kroegenes, J., Bartl, J., Bracchi, T., and SaeTRAN, L., "Aerodynamic Performance of the NREL S826 Airfoil in Icing Conditions at Low Reynolds Numbers," *Unpublished manuscript*.
- [19] Federal Aviation Administration, "14 CFR Parts 25 and 29, Appendix C, Icing Design Envelopes," DOT/FAA/AR-00/30, 2002.
- [20] Shin, J., and Bond, T. H., "Experimental and computational ice shapes and resulting drag increase for a NACA 0012 airfoil," *5th Symposium on Numerical and Physical Aspects of Aerodynamic Flows*, 1992, pp. 0–11.
- [21] Somers, D. M., "The S825 and S826 Airfoils," NREL/SR-500-36344, 2005.
- [22] Makkonen, L., "Models for the growth of rime, glaze, icicles and wet snow on structures," *Philosophical Transactions of the Royal Society of London A: Mathematical, Physical and Engineering Sciences*, vol. 358, 2000, pp. 2913–2939.